Shallow Water Seafloor Inversion using Ship-generated Striation Patterns

Paul A. Clarke (1) and Adrian D. Jones (1)

(1) Defence Science and Technology Organisation, P.O. Box 1500, Edinburgh, SA 5111, Australia

ABSTRACT

The accuracy of transmission loss model predictions in a shallow water environment is typically highly dependent on the acoustic reflectivity of the seafloor. Using sediment type databases can help determine the seafloor reflectivity, but a lack of data and conversion to acoustic properties limits reflectivity estimation accuracy. A method of inferring the seafloor reflectivity from the striation pattern produced by a ship as it transits past a hydrophone is demonstrated. This method expands on a technique devised previously (Jones and Clarke, Proceedings of 20th Intl. Congress on Acoustics, ICA 2010) in which seafloor reflectivity was inferred from multi-path interference of broadband, including impulsive, transmissions. This paper discusses the application of the striation-based method to ship data obtained from a trial conducted in shallow water off Perth, Western Australia. This includes comparisons of measured transmission loss with transmission loss model predictions using (i) sediment grabs, (ii) the impulsive inversion technique, and (iii) the striation-based inversion technique.

INTRODUCTION

Accurate prediction of acoustic Transmission Loss (*TL*) is important in regard to underwater detection by acoustic means. In shallow water (which includes most continental shelves) the seafloor reflectivity can be a critical parameter for accurate *TL* modelling, as this paper will show. Seafloor reflectivity can be obtained using sediment databases, but this is limited to the accuracy of the database for which sampling may be sparse and is typically limited to surficial sediment data.

The Defence Science and Technology Organisation (DSTO) has, for a number of years, been working on a technique to invert seafloor reflectivity using broadband sounds, to improve the *TL* prediction accuracy. This technique uses the variability in energy with frequency, termed "spectral variability", recorded several kilometres from the sound source. Since producing a broadband sound requires specific equipment, an alternative method using a passing ship's radiated acoustic signature was investigated, as this contains a high amplitude broadband component. To assist with validation of the technique, at-sea data was collected off Rottnest Island, Western Australia, with the help of Curtin University (Duncan 1999; Collins and Cahill 2003).

This paper will explain the trial setup, discuss the inversion theory, and show the results for the benchmark *TL* data and inversion using impulsive data. Next, the striation inversion method and results will be covered. Finally, the paper will show a *TL* comparison using sediment data, the impulsive inversion and the ship striation inversion.

TRIAL LOCATION AND SETUP

The trial was located in shallow water, approximately 40 m deep, just north of Rottnest Island, WA (Figure 1), with measurements taken over two days.

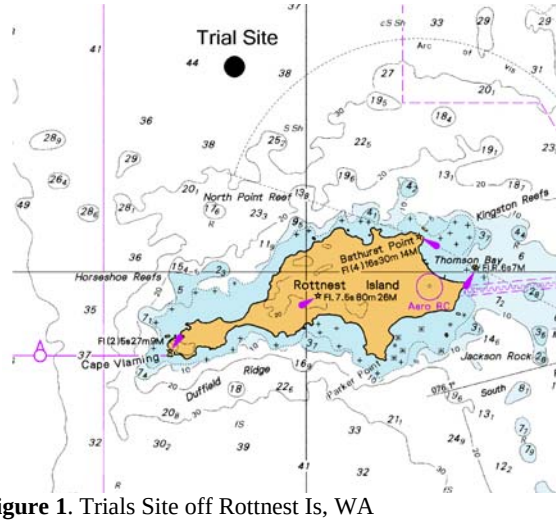

Figure 1. Trials Site off Rottnest Is, WA

The trial equipment consisted of the following:

- a broadband impulsive 20 cubic inch airgun source nominally operating at 10 m below the surface, to benchmark the *TL* of the environment and produce sounds at suitable levels for inversion using spectral variability
- a Van Veen surficial sediment grab to simulate a sediment database
- a GPS recorder to assess positions
- a CTD probe to obtain sound speed profiles of the water column
- a recorder placed on the seafloor, with a single hydrophone 8 m above the seafloor, to record the acoustic transmissions from the airgun and trials vessel
- and a trials vessel to simulate a passing ship.

During the trial a number of runs were done in straight lines past the recording post (see Figure 2) either with the airgun deployed (producing impulsive sounds) or at high speed emitting a loud ship signature (suitable for striation inversion). The maximum range for each run was 4.5 km away from the recording post. The 10 km run south was neither a high speed nor airgun run.

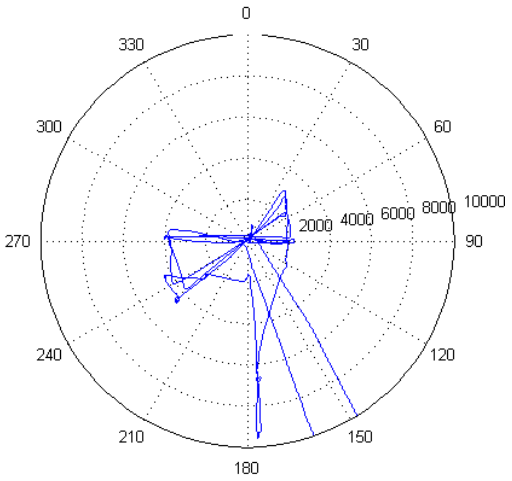

Figure 2. GPS track of the support vessel on day 1, relative to the recording post. Ranges in metres, North at 0°.

The seafloor around the trials site was relatively flat, at 40m depth, allowing range independent acoustic modelling to be done. The sea state was between 0 and 1, so the sea surface was modelled as a pressure release boundary with no reflection loss.

BACKGROUND AND BENCHMARK DATA

To check the inversion results, the *TL* at the site must be known to a reasonable accuracy. Since the airgun is a relatively stable source (if the depth and pressure are not changed) it was used to benchmark the *TL* of the environment. Airgun impulsive signals from one run were filtered into 1/3rd octave bands, using FFT processing. Background noise was also measured before each impulse.

Since the airgun Source Level (*SL*) has the potential to change significantly between deployments, due to depth and pressure changes (Duncan 1999), an estimate was made of the airgun *SL* for each 1/3rd octave band for the run. The purpose of this was so that signals received from the airgun at various range values might be processed to determine the benchmark *TL*. The *SL* estimates were based on a least-squares fit of the signal data received at short range (less than 500 m) to a model of transmission of the form $TL = A\log(\text{range})$. As the air gun data were received on a calibrated hydrophone, an absolute *SL* was obtained as the extrapolated level received at 1 m range. The value of the range exponent *A* for each 1/3rd octave was obtained as a fit to *TL* predictions from ORCA[1] generated for the first 500 m in range. The fitment was achieved by expressing these *TL* predictions from ORCA on a logarithmic range scale (on which $A\log(\text{range})$ data form a straight line) and obtaining the value of *A* from the slope of the matching straight line. Over the range 0 to 500 m, it was confirmed that spreading losses greatly dominate seafloor losses[2], so that the choice of seafloor properties for use in ORCA within this range was not critical. For convenience, ORCA was run with parameters describing the seafloor as a medium sand half-space, and values of *A* were determined for the different 1/3rd octave bands. These derived values of *A* were less than the value $A = 20$ expected for spherical spreading, but not greatly so. Using the *SL* values obtained by this process, the benchmark *TL* data, were simply obtained as the difference between the *SL* and the signal level, in dB, received at each range.

Contamination of the benchmark results by background noise was checked by putting each noise measurement, just before the airgun impulse, through the same 1/3rd octave processing (see Figure 5, blue line). Since the background level was changing in time, due to the trial vessel location relative to the receiver post, a sliding twenty sample window was applied to the background noise (see Figure 5, black line). Any benchmark sample that was within 6 dB of the background noise was marked as contaminated and rejected from further analysis. This gave a minimum 6 dB signal to noise ratio for any benchmark data.

SPECTRAL VARIABILITY

Spectral variability is the variation in the amplitude level of the phase-coherent sound pressure signal sensed at a fixed receiver, after transmission along multiple paths from a fixed source, due to a change in the signal frequency (Jones and Bartel 1998). A statistic of the frequency scale of the amplitude variability, represented as a frequency displacement Δf_h, may be shown to be related to the characteristics of the impulse response of the transmission scenario. Importantly, a measurement of this statistic may be inverted to indicate seafloor reflectivity. Detailed discussions about the theory of the spectral variability inversion technique can be found elsewhere (Jones and Clarke 2010 and 2011), so only a summary of the technique is given in this paper.

The spectral variability technique assumes a white noise broadband source. If this broadband sound travels through a shallow ocean, it is modified by the multipath environment, including seafloor and sea surface interactions (losses). These interactions "colour" the sound received at a distance from the source in accordance with the sound channel transfer function, giving variability to the observed spectral pattern. For many circumstances, it may be assumed that the seafloor losses greatly exceed surface losses and that the spectral variability is related to the former, only. For small grazing angles of incidence relevant to shallow water transmission, a reasonable approximation to the bottom loss (in dB) versus grazing angle function is that it is linear, as $F\,\beta$ dB, where *F* dB/radian is the "bottom loss function" and β the grazing angle. Using such a representation of seafloor bottom loss with grazing angle, as shown in Figure 3, the value of the bottom loss function can be calculated directly from the spectral variability of the received broadband signal (Jones and Clarke 2011).

This bottom loss straight-line assumption is a good approximation at shallow grazing angles (Jones et al. 2008; Jones, Day and Clarke 2008). A reasonable estimate for the phase change associated with this bottom loss function is illustrated

[1] ORCA is a phase coherent *TL* model based on normal mode theory (Westwood, E. K. et al., 1996).

[2] Predictions of *TL* from ORCA to 500 m range, using the trials site sound speed profile and water depth, were found to be insensitive to modelled sediment properties.

in Figure 4. Here, it is assumed that the reflection phase varies linearly with grazing angle, reaching 0° at a grazing angle corresponding with the seafloor critical angle β_c, which for a lossy seafloor is assumed to correspond with a bottom loss of, very approximately, 6 dB (Jones, Day and Clarke 2008). This is relevant if predictions of phase coherent *TL* are to be carried out using the value of *F* dB/radian obtained from an inversion such as described in this paper, but is otherwise not used in the inversion process.

To be assured that grazing angles are small, and so that the inversion may proceed using the authors' technique, the distance from the source to receiver needs to be greater than, very approximately, about thirty times the water depth (Jones et al. 2012). Also, an upper limit on the range exists due to vertical refraction in the water column, which is ignored in the technique. Typically this exceeds the "small angle" range requirement. A more detailed consideration of these limitations, and others, is given by Jones et al. (2012).

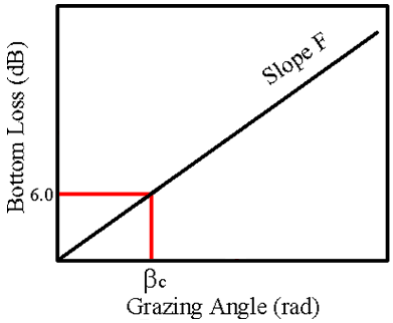

Figure 3. Bottom loss assumption used in the spectral variability calculations.

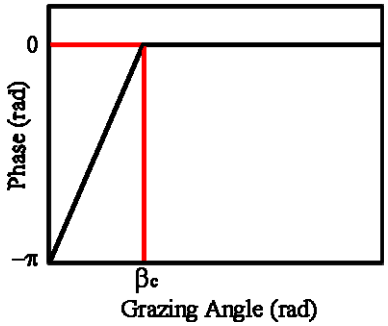

Figure 4. Bottom reflection phase assumption used in the spectral variability calculations.

This bottom loss slope, *F*, can be calculated from the spectral interference pattern using:

$$F \approx \frac{27.3 D \Delta f_h}{c_w} \text{ dB/radian} \qquad (1)$$

where Δf_h = frequency displacement at a 0.5 crossing of the sound pressure amplitude autocorrelation using the spectral interference pattern, Hz.

c_w = average sound speed in the water column, m/s.

D = depth of water, m.

It may be noted that the value Δf_h is range-independent, so long as range requirements are met, and refraction is ignored. The spectral variability technique has been tested using modelled data for two different layered seafloors (Jones, Bartel, Clarke and Day 2000), airgun impulsive sources (Jones, Hoffman and Clarke 2000) and small explosive charges as impulse sources (Jones et al. 2002; Jones and Clarke 2011). The assumption of a broadband white noise source was not relevant for the modelled data (as a flat input spectrum was employed) and can be obtained from impulsive data with some simple filtering. A ship signature is more complex, with tonals and shaped broadband noise, so its suitability as a broadband source required further investigation.

INVERSION USING BENCHMARK DATA

The *TL* benchmark data were inverted to obtain a best-fit value of the bottom loss parameter *F* dB/radian, to show how precisely any modelled results could match the benchmark data. This was done by using the KRAKENC acoustic model (Porter and Reiss 1984 & 1985) to calculate the *TL* for any seafloor reflectivity *F* dB/radian[3], and then adjusting the seafloor reflectivity until the mean KRAKENC-modelled *TL* matched the benchmark *TL*. To simulate the 1/3rd octave bands, the KRAKENC model was run at 21 different frequencies over each 1/3rd octave band during the inversion, with the results incoherently averaged. The result for 500 Hz is shown in Figure 5 against the benchmark data, with all the calculated 'best-fit' seafloor reflectivities shown in Table 1.

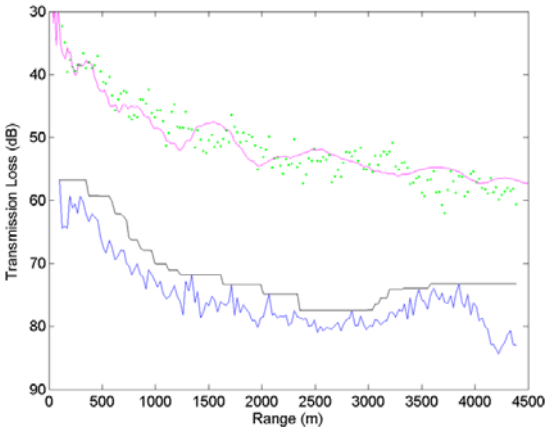

Figure 5. *TL* predictions from KRAKENC using seafloor description based on best-fit seafloor reflectivity *F*, 500 Hz. Magenta line is KRAKENC *TL*, Green points are benchmark *TL* data from one airgun run, blue line is background noise relative to the *TL* and black line is the relative background noise level used to determine the signal to noise ratio.

Table 1. Best-fit seafloor reflectivity results derived from the benchmark data.

Freq (Hz)	Seafloor reflectivity (*F* dB/rad)
63	1.5
125	3.4
250	5.3
500	4.6
1000	13.3
2000	40.1

[3] KRAKENC was run using a bottom loss vs grazing angle curve and reflection phase vs grazing angle curve, with these values obtained from *F* as shown in Figures 3 and 4.

INVERSION USING THE IMPULSIVE TECHNIQUE

Inversion of the impulsive airgun source using spectral variability was done for one run. Here, a value of Δf_h was obtained from the airgun signal at a particular range, and the seafloor reflectivity F dB/radian determined from Equation (1). This gave multiple results since a number of airgun shots were made per run, and as a value of Δf_h may be determined at each range. Figure 6 shows the reflectivity results at 500 Hz, with the inversion based on those green dots being within the required inversion ranges[4]. The seafloor reflectivity values for 1/3rd octave bands from 63 Hz to 2 kHz are shown in Table 2.

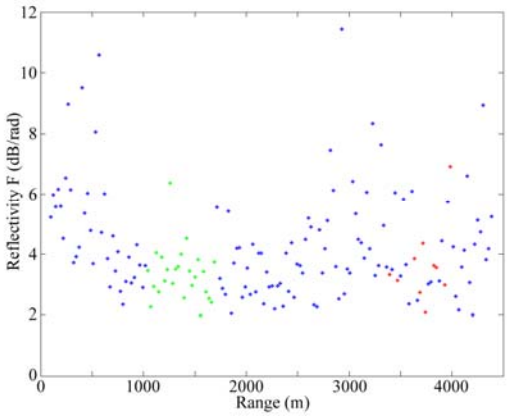

Figure 6. Reflectivity results for 500 Hz from one airgun run. Green points show valid data within the required range, blue points have an inappropriate range and red points are noise corrupted. Only the green points were used for further analysis.

Table 2. Seafloor reflectivity results derived from the airgun impulsive data.

Freq (Hz)	Seafloor reflectivity (F dB/rad)			
	Mean	STD	Min	Max
63	1.6	0.3	0.9	2.0
125	2.3	0.5	1.4	3.6
250	2.2	0.4	1.6	3.4
500	3.4	0.9	2.0	6.4
1000	3.6	1.3	1.6	6.6
2000	14.7	-	14.7	14.7

The seafloor reflectivity results from the airgun data were used as input, as shown in Figures 3 and 4, in KRAKENC and *TL* predictions compared to the benchmark data, with 21 frequencies over each 1/3rd octave used to simulate the 1/3rd octave band during modelling. The 125 and 500 Hz results are shown in Figures 7 and 8. The red lines show the maximum and minimum reflectivity results, while the green line is using the mean seafloor reflectivity and benchmark *TL* values are shown as green dots. The mean inversions show a good agreement to the benchmark *TL*, with the maximum and minimum curves showing reasonable agreement.

[4] Between thirty and fifty times the water depth was used as the required ranges for this paper.

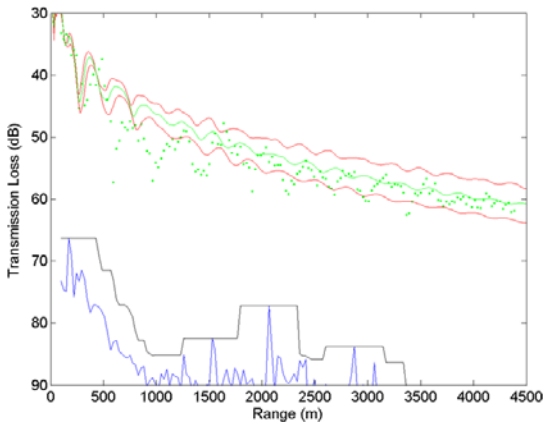

Figure 7. Modelled KRAKENC *TL* for mean, maximum & minimum airgun inverted reflectivity values at 125 Hz, shown as green & red lines. Green points are benchmark *TL* data, blue and black lines are background noise corruption checks.

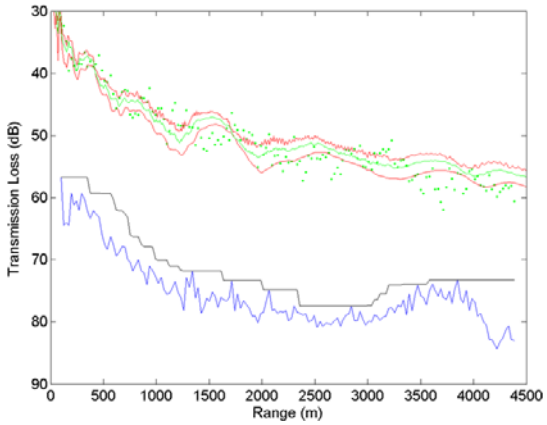

Figure 8. Modelled KRAKENC *TL* for mean, maximum & minimum airgun inverted reflectivity values at 500 Hz, shown as green & red lines. Green points are benchmark *TL* data, blue and black lines are background noise corruption checks.

INVERSION USING THE STRIATION TECHNIQUE

Using the spectral variability analysis technique on unaveraged data from the ship was tested, but the tonal part of the ship signature corrupted the spectral pattern. Temporal averaging (along lines of constant frequency) showed no improvement, since the ship tonals were unchanged and the striation pattern is not constant with range[5] (see time-frequency plot in Figure 9). A method of averaging along the lines of the striations (in place of the lines of constant frequency) was devised, since these were found to follow straight lines from the point on the range-frequency plot at which both range and frequency are zero (near CPA (closest position of approach)). As the tonals were near constant in frequency (only a very small Doppler frequency change), it was surmised that such "matched-slope" averaging would suppress the tonals while enhancing the striation interference pattern that contains the environmental component required

[5] Time was converted to range using GPS data. Since the ship had a constant speed and CPA was near the recorder buoy, conversion from time to range was approximatly linear.

for spectral inversion. The highlighted section in Figure 9 shows the required range needed for spectral inversion.

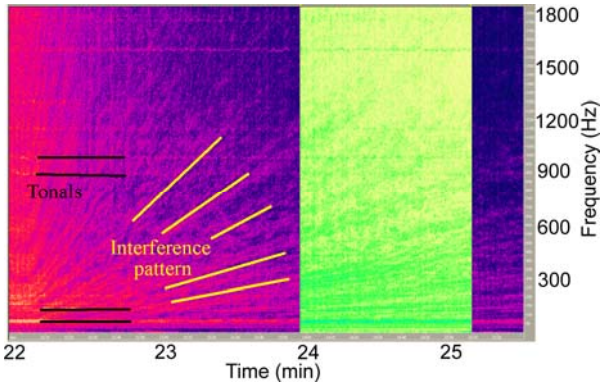

Figure 9. Spectrogram of the trials ship as it passes by the hydrophone. Ship tonals and striation interference pattern are highlighted. Time was converted to range using GPS data.

Since the striation pattern exhibited a very close adherence to the function $\Delta f / \Delta r = f / r$, it was assumed that it followed this form exactly, for purposes of data averaging.

Table 3 displays the results of averaging along the striation pattern in the spectral variability inversion. Since only one value of seafloor reflectivity, per 1/3rd octave band, is obtained per run, a number of trial vessel runs past the hydrophone were needed to investigate any variability in results using the striation inversion technique.

Table 3. Seafloor reflectivity results derived from inversion of the trials vessel striation pattern.

Freq (Hz)	Seafloor reflectivity (*F* dB/rad)			
	Mean	STD	Min	Max
63	1.6	0.5	0.8	2.5
125	2.6	0.7	1.7	3.9
250	3.1	0.5	2.4	4.3
500	6.3	1.5	4.0	10.2
1000	11.3	2.8	7.4	15.4
2000	20.3	8.1	4.7	37.2

The seafloor reflectivity results from Table 3 were used as input in KRAKENC and the *TL* predictions compared to the benchmark data, with 21 frequencies over each 1/3rd octave. Good agreement was obtained between the mean predicted *TL*, inverted from the striations, and the benchmark *TL* data, as seen in Figures 10 and 11. The minimum and maximum predicted *TL* still had reasonable agreement, but at 2 kHz the variability in seafloor reflectivity derived was large, believed due to noise corruption. Jones et al. (2012) describe the striations-based inversion process in more detail and discuss its limitations more fully.

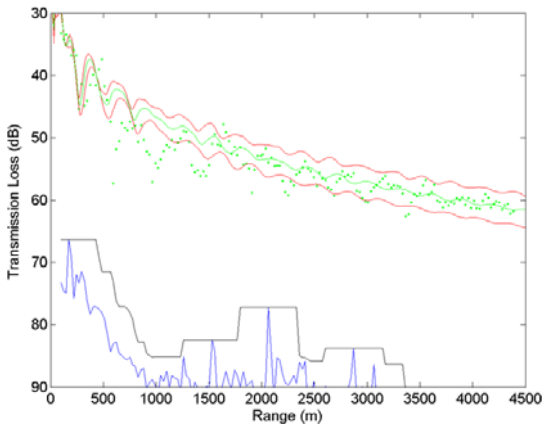

Figure 10. Modelled KRAKENC *TL* for mean, maximum & minimum striation-inverted reflectivity values at 125 Hz, shown as green & red lines. Green points are benchmark *TL* data, blue and black lines are background noise corruption checks.

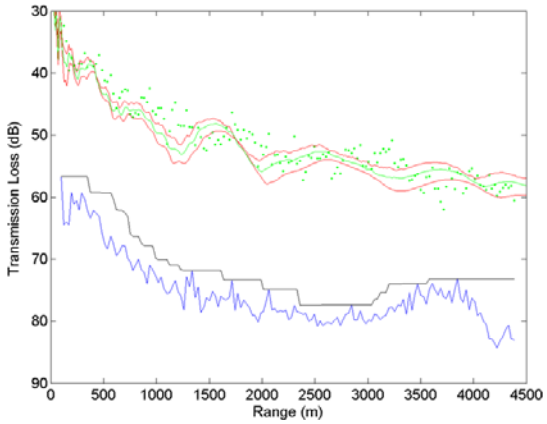

Figure 11. Modelled KRAKENC *TL* for mean, maximum & minimum striation-inverted reflectivity values at 500 Hz, shown as green & red lines. Green points are benchmark *TL* data, blue and black lines are background noise corruption checks.

TRANSMISSION LOSS USING SEDIMENT GRABS

A *TL* comparison between the airgun benchmark data and that obtained using a sediment database as input was considered useful since such databases are frequently the only source of seafloor data. In lieu of using an actual database, it was decided to obtain seafloor samples using sediment grabs taken at the site and infer this as a sediment database with good local knowledge.

The sediment grabs taken during the trial showed the study area to be relatively uniform, consisting of moderately well sorted, rounded, medium grained sand (Collins and Cahill 2003), with an average grain size of 0.93 phi[6]. The medium sand description was converted to geoacoustic properties, using approaches described by Richardson (1997) and Jensen et al. (1994), and then modelled with KRAKENC as a uniform halfspace, with 21 frequencies per 1/3rd octave. The agreement with the airgun benchmark *TL* was reasonable

[6] phi value (ϕ), where $\phi = -\log_2 d \approx -1.44 \ln d$, where d is diameter of the material grains in mm. It is common for grain size to be referenced as $n\phi$, eg. 0 ϕ is for grain size 1 mm.

over the short range shown, but it can be seen that the modelled *TL* has under predicted at 4 km by a few dB, which could likely result in a larger error at longer ranges.

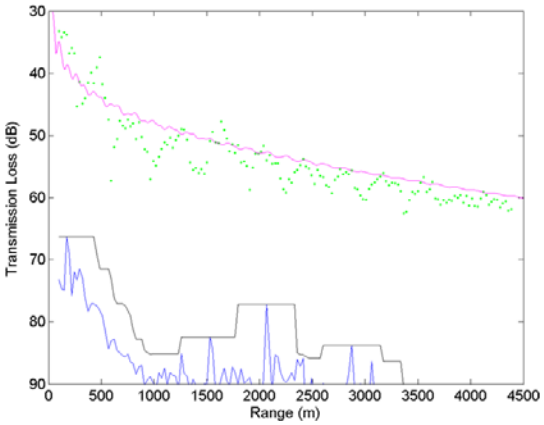

Figure 12. *TL* predictions using sediment data modelled at 125 Hz. Green points are benchmark *TL* data; Magenta line is *TL* modelled using KRAKENC; blue and black lines are background noise corruption checks.

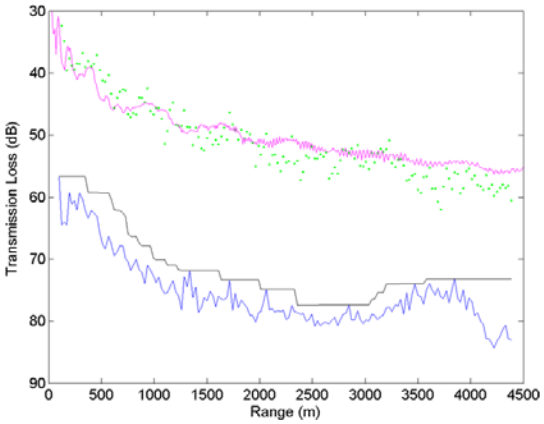

Figure 13. *TL* predictions using sediment data modelled at 500 Hz. Green points are benchmark *TL* data; Magenta line is *TL* modelled using KRAKENC; blue and black lines are background noise corruption checks.

COMPARISON OF METHODS USING RANGE OF THE DAY

A comparison between the best-fit seafloor reflectivity and inverted seafloor reflectivities, for the striation and impulsive inversions, is possible but an alternative metric is predicted sonar system performance 'detection ranges'. Also, no seafloor reflectivity was calculated from the sediment grabs. Comparisons of transmission losses to benchmark data could only show results to 4.5 km, since this was the benchmark range obtain during the at-sea trial, whereas detection ranges of interest can exceed this range.

So, to obtain comparisons at larger ranges the best-fit *TL*, using benchmark data, was assumed correct. Detection Range Of the Day (*ROD*) detection ranges were then set to 5, 10 and 20 km for this best-fit *TL* and a simulated passive sonar figure of merit (e.g. Urick 1983) obtained for each range and frequency. This figure of merit could then be used to calculate the passive *ROD* for each inversion type and frequency.

The calculated passive *ROD* values can be seen for each inversion type at ranges 5, 10 and 20 km in Tables 4, 5 and 6. Since the errors are not obvious in these tables they were converted to percentage errors, and are shown in Tables 7, 8 and 9. This shows a modest *ROD* average error of 20% for inversions using the striation data, a 28% *ROD* average error for inversions using the impulsive data, and a larger 90% *ROD* average error using acoustic properties derived from the sediment data.

Table 4. Range Of The Day for seafloor reflectivities inverted from the impulsive data.

Freq (Hz)	Expected *ROD*		
	5 km	10km	20km
	ROD using inverted data (km)		
63	4.7	9.4	18.6
125	6.3	13.2	27.4
250	7.8	16.4	35.3
500	5.2	11.0	23.3
1000	5.8	14.5	32.5
2000	6.4	11.2	21.0

Table 5. Range Of The Day for seafloor reflectivities inverted from the trials vessel striation pattern.

Freq (Hz)	Expected *ROD*		
	5 km	10km	20km
	ROD using inverted data (km)		
63	4.7	9.4	18.6
125	5.8	12.1	24.9
250	6.5	13.6	28.5
500	3.9	8.0	16.7
1000	3.6	10.5	21.6
2000	6.3	10.9	19.8

Table 6. Range Of The Day using a seafloor description based on sediment grabs.

Freq (Hz)	Expected *ROD*		
	5 km	10km	20km
	ROD (km)		
63	8.7	19.7	41.8
125	10.0	22.7	50.8
250	9.4	20.8	46.6
500	6.2	14.3	32.8
1000	7.9	17.5	39.0
2000	10.2	20.2	32.8

Table 7. Range Of The Day error for seafloor reflectivities inverted from the impulsive data.

Freq (Hz)	Expected *ROD*		
	5 km	10km	20km
	ROD error using inverted data (%)		
63	6	7	7
125	27	32	37
250	56	64	77
500	4	10	17
1000	16	45	63
2000	28	12	5

Table 8. Range Of The Day error for seafloor reflectivities inverted from the trials vessel striation pattern.

Freq (Hz)	Expected *ROD*		
	5 km	10km	20km
	ROD error using inverted data (%)		
63	6	7	7
125	16	21	25
250	30	36	43
500	28	25	20
1000	39	5	8
2000	26	9	1

Table 9. Range Of The Day error using a seafloor description based on sediment grabs.

Freq (Hz)	Expected *ROD*		
	5 km	10km	20km
	ROD error (%)		
63	74	97	109
125	100	127	154
250	88	108	133
500	24	43	64
1000	58	75	95
2000	104	102	64

CONCLUSIONS

Comparison of the three calculated sets of seafloor reflectivity data which were inverted from benchmark data, impulsive data and striations, shows a good correlation for both the mean impulsive and striation inversion results to the benchmark data. There is significant variability in results, at each frequency, for both inversion methods and therefore some averaging is recommended.

The *TL* predictions using spectral variability inversions from impulses or striations have improved correlation to the benchmark data, compared to using sediment grabs. However all techniques gave reasonable *TL* predictions at this location. Averaging over a number of inversions again improves the predictions.

The *ROD* comparison demonstrated how small *TL* errors can manifest into larger *ROD* prediction errors and this was highlighted by the differences using the sediment grab technique.

ACKNOWLEDGEMENTS

This work would not have come to pass without the assistance of the following people:

- Dr. Alec Duncan, Mr. Malcolm Perry, and Prof. Sasha Gavrilov from Curtin University for their help with trial planning and during the trial;
- Prof. Lindsay B. Collins and Mr. Quinton Cahill from Curtin Uni for obtaining the sediment samples and analysis of these sediments;
- The crew of MV Total Warrior for their assistance during the trial.

REFERENCES

Collins, Lindsay B. and Cahill, Quinton 2003, *Experimental Validation on In-situ Seafloor Reflectivity Measurement technique, Sediment and Substrate Characteristics in part of the "Approaches to Fremantle"*, Curtin University of Technology, Report DAG 1.22.07.03, May 2003.

Duncan, A.J. 1999, *Research into the Acoustic Characteristics of an Air-gun Sound Source*, CMST, Curtin University, Report C99-12, July 1999

Duncan, A.J. 2003, *Experimental Validation on In-situ Seafloor Reflectivity Measurement technique*, Curtin University of Technology, CMST, Project CMST 419, Report C2003-05, May 2003.

Jensen, F.B, Kuperman, W.A., Porter, M.B., and Schmidt, H. 1994, *Computational Ocean Acoustics*, American Institute of Physics.

Jones, A.D. and Bartel, D.W. 1998, *Spectral Variability in a Shallow Water Environment*, UDT Pacific 98 Conference, Darling Harbour, Sydney, Australia, 24-26 February 1998.

Jones, A.D., Bartel, D.W., Clarke, P.A., and Day, G.J. 2000, *Acoustic Inversion for Seafloor Reflectivity in Shallow Water Environment*, UDT Pacific 2000, Darling Harbour, Australia, 7-9 February 2000.

Jones, A.D., Hoffman, J., and Clarke, P.A., 2000, *Seafloor Reflectivity – A Test of an Inversion Technique*, Proceedings of Australian Acoustical Society Annual Conference 2000, Joondalup, Western Australia, 15 – 17 November 2000.

Jones, A.D., Sendt, J.S., Zhang, Z.Y., Clarke, P.A. and Exelby, J.R. 2002, *Optimisation of Transmission Predictions for a Sonar Performance Model for Shallow Ocean Regions*, Proceedings of Australian Acoustical Society Annual Conference 2002, Adelaide, South Australia, 13 – 15 November

Jones, Adrian D., Sendt, Janice, Duncan, Alec J., Clarke, Paul A. and Maggi, Amos L. 2008, *A Comparison of Sonar Transmission Models at Mid-Frequency for Downward Refracting Shallow Oceans*, UDT Pacific 2008, Sydney, Australia.

Jones, A.D., Day, G.J. and Clarke, P.A. 2008, *Single parameter description of seafloors for shallow oceans*, Proceedings of Acoustics'08 Paris, Paris, France, 29 June – 4 July 2008, pp 1725 – 1730, also published in Proceedings of the 9th European Conference on Underwater Acoustics, ECUA 2008, Volume 1, pp 161 – 166.

Jones, A.D. and Clarke, P.A. 2010, *Rapid seafloor inversion in shallow oceans using broadband acoustic data*, Proceedings of 20th International Congress on Acoustics, ICA 2010, Sydney, Australia, 23-27 August

Jones, A. D. and Clarke, P. A. 2011, *Seafloor Inversion for Shallow Oceans Using Broadband Acoustic Data*, Proceedings of 4th International Conference and Exhibition on Underwater Acoustic Measurements: Technologies & Results, Kos, Greece, 20-24 June, pp 9 – 14

Jones, Adrian D., Bartel, David W. and Clarke, Paul A. 2012, *An Application of Range-Frequency Striations to Seafloor Inversion in Shallow Oceans*, Acoustics 2012, Australian Acoustical Society Annual Conference, Fremantal, WA.

Porter, Michael B. and Reiss, Edward L., (1984), *A numerical method for ocean-acoustic normal modes*, JASA 76, 244-252.

Porter, Michael B. and Reiss, Edward L. 1985, *A numerical method for bottom interacting ocean acoustic normal modes*, JASA 77, 1760-1767 (1985).

Richardson, M. D. 1997, *In-Situ Shallow Water Sediment Geoacoustic Properties*, International Conference on Shallow Water Acoustics, Beijing China, April 1997

Urick, R.J. 1983, *Principles of Underwater Sound*, 3rd edition, Peninsula Publishing, Los Altos

Westwood, E. K., Tindle, C. T., and Chapman, N. R. 1996, *A normal mode model for acousto-elastic ocean environments*, J. Acoust. Soc. Am., 100, 3631-3645.